IEEE Access
Multidisciplinary | Rapid Review | Open Access Journal

Received September 8, 2020, accepted September 16, 2020, date of publication September 18, 2020,
date of current version September 30, 2020.

*Digital Object Identifier 10.1109/ACCESS.2020.3025052*

# Uncertainty Quantification for SAE J2954 Compliant Static Wireless Charge Components

**VINCENZO CIRIMELE[1], (Member, IEEE), RICCARDO TORCHIO[2], JUAN LUIS VILLA[3], FABIO FRESCHI[1], (Senior Member, IEEE), PIERGIORGIO ALOTTO[2], (Senior Member, IEEE), LORENZO CODECASA[4], (Senior Member, IEEE), AND LUCA DI RIENZO[4], (Senior Member, IEEE)**

[1]Department of Energy "G. Ferraris", Politecnico di Torino, 10129 Turin, Italy
[2]Dipartimento di Ingegneria Industriale, Università degli Studi di Padova, 35131 Padova, Italy
[3]Departamento de Ingeniería Eléctrica, CIRCE, Universidad de Zaragoza, 50009 Zaragoza, Spain
[4]Dipartimento di Elettronica, Informazione e Bioingegneria, Politecnico di Milano, I-20133 Milan, Italy

Corresponding author: Riccardo Torchio (riccardo.torchio@unipd.it)

The work of Riccardo Torchio was supported by the Università degli Studi di Padova, Italy, BIRD 2019 program, under Grant BIRD 195949/19.

**ABSTRACT** The present work aims at quantifying how, and how much, the uncertainties on the components and material parameters of a wireless power transfer (WPT) system for the static charge of electric vehicles affect the overall efficiency and functionality of the final produced device. With the aim of considering the perspective of a possible industrial developer, the parameters selected for the uncertainty quantification are chosen to be the capacitance values of the compensation capacitors and the electromagnetic material parameters used for the construction of the magnetic structure of a WPT system, i.e. the parameters of the elements to be purchased. The analysis is based on a standard system among the ones provided by the current SAE J2954 recommended practice.

**INDEX TERMS** Wireless power transmission, inductive power transmission, uncertainty quantification, parametric model order reduction, compensation capacitors.

## I. INTRODUCTION

After about two decades of growing research interest in wireless charging systems for electric vehicles (EVs), the technology of recharging by means of resonant coupled inductors, commonly referred to as wireless power transmission (WPT), is capturing the interest of the automotive industry [1]–[10]. Indeed, various companies are developing their own products for the static charging, i.e. the charging taking place when the vehicle is not moving and the misalignment is constrained within a defined limit.

Various authors have proposed different structures for power electronics on ground and on board the vehicle [11]–[16]. Also the working frequency of the converters has been widely debated, as well as the control techniques. For example, [14] presents a 1 kW system for static charge based on a variable frequency control around a rated frequency of 20 kHz. Authors of [15], instead, indicate a 7 kW system working with a fixed frequency control at the rated frequency of 79 kHz. At the same time, various researchers have proposed different structures and shapes for the coils and each of these solutions has distinctive features, such as robustness to misalignment, reduction of the stray magnetic field, cost effectiveness, etc. [17]–[20]. However, in recent years, standardization processes have led to the definition of precise characteristics for static WPT systems applied to the charging of light-duty electric vehicles. Among these, the SAE J2954 Recommended Practice (RP) [21] provides a precise classification of WPT systems based on rated power level and distance between the coils, indicating also a precise working frequency range. At the same time, the SAE J2954 RP also provides some examples of coil structures and reference structures to be used as test stands for characterization and interoperability analysis.

The existence of this RP makes precise indications for the implementation of WPT systems available, thus expanding the pool of possible developers. However, the production of such kind of systems aimed at marketing, calls for attention

The associate editor coordinating the review of this manuscript and approving it for publication was Leandros Maglaras.

on several aspects which are related to manufacturing tolerances. In fact, as with all electrical machines, the performances of WPT systems can be subject to uncertainty linked to the manufacturing tolerances of materials and components. From the perspective of an industrial developer, it is important to quantify how the choice on the components to be purchased, and thus their uncertainties, will affect the performances of the WPT system from a statistical point of view. Recent work [22] addressed this issue by considering a small WPT device for extremely low power mounted on a Printed Circuit Board (PCB). However, despite its great importance in the industrial sector, to the best of the authors' knowledge, uncertainty quantification aspects have been poorly treated in the literature concerning EVs charging applications.

For this reason, the present work aims at addressing and quantifying the effects of tolerances by evaluating their effects on the system performances. The study is conducted around test bench and reference coil assemblies described in the SAE J2954 RP and focuses on the tolerances related to the electromagnetic characteristics of materials and the value of compensation capacitors. The economical consequences of such tolerances are indeed not negligible since the cost of ferrite and capacitors constitutes a significant part of the overall cost of WPT systems. Geometrical tolerances are instead not considered since the typical manufacturing processes related to the construction of the magnetic structure assembly make their effects on the uncertainty negligible [23]–[25].

The main contribution of the work consists in the presentation of an accurate uncertainty quantification analysis to determine how the performance of realistic WPT systems (based on the SAE J2954 RP) can be affected by the tolerances of the main components. This type of analysis is of great interest especially in relation to a real system implementation and on an industrial scale. In this case, cost reduction is crucial and our work indicates precisely which components can, or cannot, be exceeded in terms of tolerance and to what extent. Moreover, it is worth noting that the numerical method developed to perform the uncertainty quantification allows for taking into account *simultaneously* electromagnetic fields and lumped circuit parameters. In addition, the adoption of Model Order Reduction allows for performing the uncertainty quantification in a very accurate way and with a computational cost significantly reduced with respect to conventional simulation techniques. Thus, in the presented uncertainty quantification analyses the whole electromagnetic problem coupled with circuit parameters has been considered, therefore without introducing approximation. In the best of the authors' knowledge, such accurate analysis based on realistic WPT systems with realistic material and components parameters and tolerances has not been presented in the literature yet.

The rest of the paper is organized as follows. Section II provides a general description of WPT systems for EVs and proposes a circuit representation of the problem. Section III presents the classifications proposed by the SAE J2954 RP and describes the WPT device adopted as reference for the present study. In Section IV, an overview of the effects of tolerances on the compensation capacitors on the WPT system performance is discussed. In Section V, the considered uncertainties and their characteristics are described. Section VI shortly describes the numerical method adopted for the uncertainty quantification of the coupled circuit–electromagnetic problem. Finally, in Section VII, the results of the analysis are presented and discussed, whereas, in Section VIII, the main outcomes of the work are summarized.

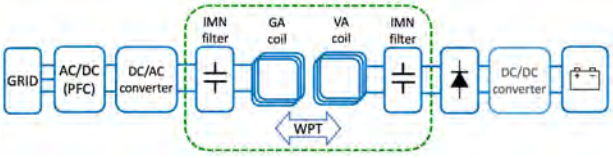


**FIGURE 1.** Scheme of the power components of WPT systems described by SAE J2954 RP. The green dashed lines encircles the objects of the analysis. Adapted from [21].

## II. GENERAL DESCRIPTION OF A WPT SYSTEM

A general scheme of a WPT system is proposed by the SAE RP. Its main power components are shown in Fig. 1. On the ground (i.e. transmitter) side, the system includes an AC/DC converter for the interface with the electric grid, having also the role of power factor corrector (PFC), a DC/AC converter, typically an H-bridge, that supplies the transmitter coil and its compensation components. On the vehicle (i.e. receiver) side, the receiver coil and its compensation components are connected to a diode rectifier and the vehicle battery. The interface with the battery can be handled by an optional DC/DC converter [21] whose presence is not considered in this study. The magnetic part directly responsible for the wireless power transmission comprises the two coils and other auxiliary electromagnetic and mechanical components whose ensembles are indicated as ground assembly (GA) and vehicle assembly (VA), respectively. The blocks that contain the compensation elements are generally indicated as impedance matching network (IMN), as they can contain one single capacitor as well as a more complex circuit consisting of several reactive components [26]–[28]. In the present case, each IMN block is considered as being constituted by a single compensation capacitor connected in series to the respective coil. This assumption simplifies the analysis and, at the same time, represents a widely adopted topology [11]–[13], [29]. Finally, it is worth mentioning that complex connection topologies between IMN and coil can in any case be represented at their terminals as the series of a capacitance and an inductance [26]. The system is doubly tuned to work under resonance condition. Moreover, the presence of the diode rectifier at the receiver side forces its input current and voltage to be in phase. Therefore, the system can be effectively represented by means of the circuit shown in Fig. 2 based on the first harmonic approximation (FHA) [29], [30]. The output of the DC/AC converter is then represented by a sinusoidal voltage source $\underline{V}_1$ while all the components connected to the receiver coil are represented by an equivalent load resistance

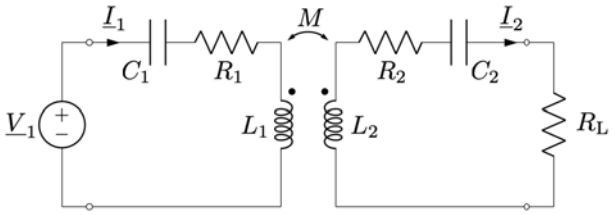


**FIGURE 2.** FHA model of the series-series compensated WPT system.

$R_L$ whose value depends on the rated battery power $P_{batt}$ and voltage $V_{batt}$ according to the following relationship:

$$R_L = \frac{8}{\pi^2}\frac{V_{batt}^2}{P_{batt}} \tag{1}$$

The factor $8/\pi^2$ is valid for series compensation of the receiver but can slightly vary for different compensation topologies [31], [32]. Transmitter and receiver coils (i.e. GA and VA coil in Fig. 1) are represented by means of the inductances $L_1$ and $L_2$, respectively, and their electromagnetic interaction is modelled through the mutual inductance $M$ [33]. Transmitter and receiver compensation capacitors are (i.e. left and right IMN filters in Fig. 1) represented through the capacitances $C_1$ and $C_2$, respectively. $R_1$ and $R_2$ represent the equivalent series resistances of the compensated coils. The two sides of the system can be then described by the following set of equations:

$$\underline{V}_1 = \left[R_1 + j\left(\omega L_1 - \frac{1}{\omega C_1}\right)\right]\underline{I}_1 - j\omega M\underline{I}_2 \tag{2}$$

$$0 = \left[(R_2 + R_L) + j\left(\omega L_2 - \frac{1}{\omega C_2}\right)\right]\underline{I}_2 - j\omega M\underline{I}_1 \tag{3}$$

In the series-series compensation topology, the capacitors are chosen on the base of the values of the self-inductances according to the relationship:

$$\omega_0^2 = \frac{1}{L_1 C_1} = \frac{1}{L_2 C_2} \tag{4}$$

where $\omega_0$ is the resonance angular frequency of the system.

For generic values of the angular frequency $\omega$, the entire system is seen from the source terminals as a *total impedance* $\hat{Z}_T$, i.e.:

$$\hat{Z}_T = R_1 + \mathrm{j}\left(\omega L_1 - \frac{1}{\omega C_1}\right) + \frac{\omega^2 M^2}{(R_2 + R_L) + \mathrm{j}\left(\omega L_2 - \frac{1}{\omega C_2}\right)} \tag{5}$$

Hence, the complex power provided by the source $\underline{S}_1$ can be expressed as:

$$\underline{S}_1 = \hat{Z}_T I_1^2 \tag{6}$$

whereas the active power $P_1$ linearly depends on real the part of the impedance $\hat{Z}_T$, i.e.:

$$P_1 = \Re\left\{\hat{Z}_T\right\} I_1^2 \tag{7}$$

while the transmitted power to the load is given by:

$$P_L = R_L I_2^2 \tag{8}$$

Hence, the efficiency of the power transmission can be expressed as:

$$\eta = \frac{P_L}{P_1} = \frac{\omega^2 M^2 R_L}{R_1\left(\omega L_2 - \frac{1}{\omega C_2}\right)^2 + R_1 (R_2 + R_L)^2 + \omega^2 M^2 (R_2 + R_L)} \tag{9}$$

When working at the resonance frequency, the terms inside the round brackets of equation (5) become equal to zero and $\hat{Z}_T$ becomes purely real. In this condition, $\underline{S}_1$ and $P_1$ are equal, meaning that the power factor (PF) of the WPT system becomes equal to one and the source has to provide uniquely active power. From the point of view of the real system of Fig. 1, when the condition (4) is respected by design, the VA rating of the DC/AC converter can be designed to correspond to the rated active power of the system. This implies that size and cost of the DC/AC switches can be greatly reduced and, at the same time, the switches can be operated in order to achieve soft-switching, i.e. by reducing the commutation losses practically to zero [34], [35].

## III. SAE INDICATIONS, CLASSIFICATION AND ADOPTED REFERENCE SYSTEM

The development of standards concerning WPT for EVs has contributed to the definition of the requirements for such kind of devices, providing at the same time a classification system and guidelines for the construction of reference magnetic structures.

Since the first publication of the J2954 standard draft, this document fixed a precise range for the resonance frequency $f_0 = \omega_0/2\pi$ corresponding to the working frequency of the DC/AC converter at the transmitter side. In the current version, the RP reads: "*for systems using frequency tuning to compensate for various operating variations, the operating frequency must remain in the range of* 79 *to* 90 kHz" [21]. This range is centered on the rated value of 85 kHz. Hence, as clearly stated, these definitions cover both cases of fixed and variable frequency regulations.

As far as the WPT systems classification is concerned, the SAE RP considers two distinctions. A first classification is based on the power classes, for which the RP proposes four *WPT-classes* that are defined in terms of the maximum input apparent power absorbed by the on-ground power electronics. The different WPT classes are detailed in Table 1. In the current version, the main requirements for WPT systems are completely defined for WPT1, WPT2 and WPT3 classes while several aspects (e.g. the requirements in terms of interoperability) are indicated as to-be-defined for the WPT4 class. A second classification is based on the *Z-classes*. Having Fig. 3 as reference, the Z classification

**TABLE 1.** WPT-class classification according to SAE J2954 [21].

| WPT1 | WPT2 | WPT3 | WPT4 |
|---|---|---|---|
| 3.7 kVA | 7.7 kVA | 11 kVA | 22 kVA |

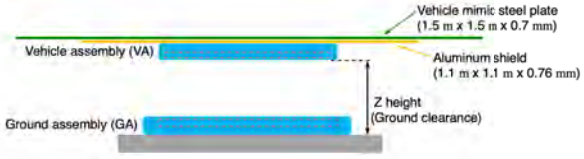


**FIGURE 3.** Sketch of the SAE J2954 RP test-bench. Adapted from [21].

**TABLE 2.** Z-class classification according to SAE J2954 RP [21].

| Z-class | Ground clearance range |
|---|---|
| Z1 | 100 mm – 150 mm |
| Z2 | 140 mm – 210 mm |
| Z3 | 170 mm – 250 mm |

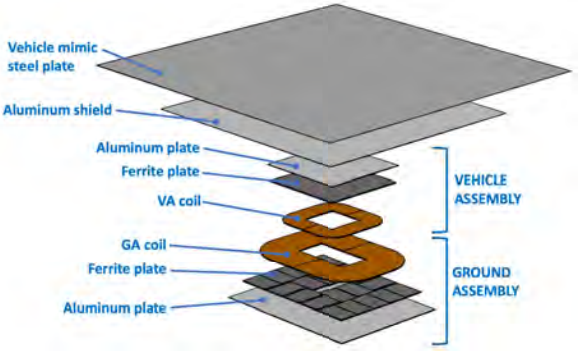


**FIGURE 4.** View of the Ground Assembly (GA) and Vehicle Assembly (VA) Test Stand WPT2 proposed by SAE J2954. The GA is equal for all Z-classes while the depicted VA refers to the Z3 class. Adapted from [21].

refers to the ground clearance of the whole vehicle assembly (VA). In this case, this classification considers three Z classes whose ranges are detailed in Table 2. Finally, the RP proposes a series of reference magnetic structures (*test-stands*) for each WPT-class (not yet defined for WPT3 and WPT4) and Z-class. These structures are proposed for the testing and assessment of commercial systems within a dedicated *test-bench* setup here described by means of the sketches of Fig. 3 and Fig. 4. Both figures refer to a WPT2/Z3 system that is used as reference for the present work.

The test-stand develops around the transmitter and receiver coils, both rectangular in shape and consisting of 8 turns of litz wire. The coils are placed on a ferrite pad which, in turn, rests on a 1 mm thick aluminum plate. When placed in the test-bench, the receiver structure (i.e. the VA) is surrounded by a 6061 aluminum shield and an ASTM A1008 steel plate whose role is to emulate the presence of the vehicle chassis [36].

Eventually, the SAE RP proposes a range for the battery voltage $V_{\text{batt}}$ to be considered when performing the compliance tests of the whole system. This range goes from $V_{\text{batt,max}} = 420$ V to $V_{\text{batt,min}} = 280$ V.

**TABLE 3.** Model derived values of self and mutual inductances of the Test Stand WPT2 GA and VA proposed by SAE J2954 for different Z-heights [21].

| Z-height | $L_1$ | $L_2$ | $M$ |
|---|---|---|---|
| 250 mm ($Z3_{\max}$) | 44.0 $\mu$H | 38.6 $\mu$H | 5.4 $\mu$H |
| 170 mm ($Z3_{\min}$) | 43.1 $\mu$H | 39.8 $\mu$H | 11.0 $\mu$H |
| **Average values** | | | |
| 210 mm ($Z3_{\text{mean}}$) | 43.6 $\mu$H | 39.2 $\mu$H | 7.7 $\mu$H |

**TABLE 4.** Comparison of the model derived values of self and mutual inductances and the values provided by SAE J2954 for the Test Stand WPT2 GA and VA [21].

| Parameter | SAE value | Model value | Relative difference |
|---|---|---|---|
| $L_{\text{GA}}$_min | 42.1 $\mu$H | 43.1 $\mu$H | 2.1% |
| $L_{\text{GA}}$_max | 43.2 $\mu$H | 44.0 $\mu$H | 1.9% |
| $L_{\text{VA}}$_min | 37.9 $\mu$H | 38.6 $\mu$H | 1.8% |
| $L_{\text{VA}}$_max | 39.0 $\mu$H | 39.8 $\mu$H | 2.0% |

A preliminary evaluation through the electromagnetic simulation of the adopted WPT2/Z3 system by means of the Partial Element Equivalent Circuit (PEEC) method [37] (see Section VI for more details) is used to compute the values of the self and mutual inductances of transmitter and receiver for different coil distances within the allowed range of the Z3 class. The analyzed heights and the resulting values are reported in Table 3. The rated conductivity values $\sigma_{Al} = 26.3$ MS/m for the 6061 aluminum and $\sigma_{Steel} = 6.85$ MS/m for the ASTM A1008 steel have been derived from available databases [38], [39]. In the case of the ferrite, the SAE RP does not provide any indication about the material neither the expected values of magnetic permeability. In this case, the relative permeability value $\mu_{\text{r}} = 2{,}000$ has been assumed, which represents a value often found in literature [23], [40], [41]. The results of the model have been assessed by comparing them with the reference values provided by the SAE RP and summarized in Table 4. The self resistances of the coils are evaluated considering the coils made of litz wire according to the method presented in [42] and result to be $R_1 = 38.5$ m$\Omega$ and $R_2 = 61.0$ m$\Omega$.

## IV. IMPACT OF TOLERANCES

Several past works, including [43]–[45], have shown how the effect of manufacturing tolerances on components can cause a substantial change in the behaviour and performance of WPT systems.

These effects have been mainly related to tolerances on capacitance values, but can also result from variations of self and mutual inductance values [45] due to tolerances on the electromagnetic parameters of the materials used in the construction of the system.

Mainly, the presence of tolerances causes strong variations in the amplitude and phase of the total impedance that can be see as deformations in the curve of the amplitude with respect to the frequency and an horizontal and vertical shift of the phase [43].

In particular, it has been highlighted how the presence of tolerances causes a shift of the resonance frequency that no longer occurs at the nominal frequency of 85 kHz. As a consequence, in case the power electronics that supplies the

system works with a variable frequency control that follows the resonance point, the working point can be reached outside the frequency range allowed by the SAE RP. Conversely, in case of fixed frequency control that maintains the working point at 85 kHz, the power electronics may be forced to handle a not negligible reactive power, with consequent increase of switching losses and size of the power electronic switches. Naturally, this reflects back on variations in the transmitted power as well as in the efficiency of the power transmission. In some cases, these effects can translate into a strong deviation from the expected performance downstream of the system design phase and even non-compliance with the limits proposed by the SAE RP. Moreover, in the case that the resonance frequency shift leads to equivalent capacitive behaviour of the total impedance, it is mandatory to adopt more complex architectures of the power electronics or silicon–carbide based technologies, which are still more expensive with respect to standard silicon based technologies [11].

It is worth mentioning that the amplitude of the aforementioned variations in the behaviour of $\hat{Z}_{\mathrm{T}}$ is strongly dependent also on variations of the voltage of the vehicle battery, here represented by means of the equivalent load $R_{\mathrm{L}}$.

The rest of the work aims at evaluating the effects of tolerances on the performance of the WPT system in *statistical terms* by considering the uncertainty in the electromagnetic parameters of the materials of the magnetic structure (e.g. the relative permeability of the ferrite plates) which are taken into account in the following analysis together with the manufacturing tolerances that affect the values of the compensation capacitors. Clearly, these effects need to be properly addressed by a simulation method which allows for coupling circuit and electromagnetic problems.

## V. ANALYZED PARAMETERS AND THEIR UNCERTAINTY

The uncertainties on the performance of the analyzed system may depend on geometric parameters (such as arrangement of the conductors, thickness and shape of the different elements) and the electromagnetic characteristics of the materials and components. In the analyzed case, the geometric uncertainties are definitely negligible. A proof of this assumption can be found in the dissertation [25] in which the measurements on 46 different manually constructed transmitter coils are presented. The measurements showed a maximum variation of the self-inductance equal to 4.1 $\mu$H over an average value of self inductance equal to 281.4 $\mu$H (i.e. a variation range of 1.46%). Therefore, in addition to the values of the compensation capacitors, the analysis of the uncertainty focuses on the electromagnetic parameters of the materials composing the system elements described in Fig. 3 and Fig. 4. These parameters are summarized in Table 5 along with their considered tolerance ranges. As widely known in practice, the tolerances on the values of the capacitors most widely commercially available are equal to 20%, but more precise and more expensive realizations can offer uncertainties of 10% or 5%. In [46], data-sheets of several capacitors produced by an important supplier of electronic components can be found. As stated, such data-sheets show that the typical value of tolerances on the value of the capacitance are, indeed, 20% 10% and 5%. Another example can be found in [47], where the data-sheet of a high voltage film capacitor similar to the one used in [48] and [49] for WPT applications is reported. The tolerances on the conductivity of aluminum and steel have been derived from the values shown in data sheets [38], [39], while the tolerance on the relative permeability value of the ferrite has been deduced from [50]. It is worth noting that, among all the components of which the resonating magnetic structure of WPT devices consists, the main parts that influence the overall cost are the ferrite cores and the compensation capacitors. In particular, the cost of the latter is directly related to their manufacturing tolerances. For commercial reasons, vendors usually do not provide such kind of economical information in the data–sheets and catalogues, but they provide such kind of information when contacted by potential buyers. For instance, the capacitor described in [51] has a 10% tolerance. However, by contacting the supplier it was possible to purchase a 5% tolerance capacitor with an increase in the cost of the capacitor of about 20%. Such capacitor was the one actually adopted in the WPT system presented in [52] by the authors. Thus, although it is difficult to give exact figures concerning the price of such components, in the authors experience, capacitors with 5% tolerance have a cost that can be up to 30% higher that of capacitors with 20% tolerance. This leads to total component cost differences of around 8% between these two options. Therefore, from the perspective of an industrial developer, an analysis to correlate manufacturing tolerance with the overall system performance is of great interest.

**TABLE 5. Parameters affected by uncertainty considered in the present work.**

| Parameter | Symbol | Nominal | Tolerance |
|---|---|---|---|
| Relative permeability ferrite transmitter | $\mu_{\mathrm{r,tr}}$ | 2,000 | $\pm 20\%$ |
| Relative permeability ferrite receiver | $\mu_{\mathrm{r,re}}$ | 2,000 | $\pm 20\%$ |
| Conductivity plate transmitter | $\sigma_{\mathrm{Al,tr}}$ | 26.3 MS/m | $\pm 15\%$ |
| Conductivity plate receiver | $\sigma_{\mathrm{Al,re}}$ | 26.3 MS/m | $\pm 15\%$ |
| Conductivity shield | $\sigma_{\mathrm{Al,sh}}$ | 26.3 MS/m | $\pm 15\%$ |
| Conductivity vehicle mimic steel plate | $\sigma_{\mathrm{Steel}}$ | 6.85 MS/m | $\pm 15\%$ |
| Value of capacitor $C_1$ | $C_1$ | $(\omega_0{}^2 L_1)^{-1}$ | $\pm 5\%, 10\%, 20\%$ |
| Value of capacitor $C_2$ | $C_2$ | $(\omega_0{}^2 L_2)^{-1}$ | $\pm 5\%, 10\%, 20\%$ |

In the adopted method, as well as in each problem taking into account the uncertainty propagation, it is necessary to assume a probability distribution for the tolerances taken into account. In practice, however, the manufacturers neither provide this information on the data sheets, nor indicate if the uncertainty is provided according to a deterministic or probabilistic method. The ISO ENV 13005 standard ''Guide to the expression of uncertainty in measurements'' suggests that, in the absence of the specification of the probability

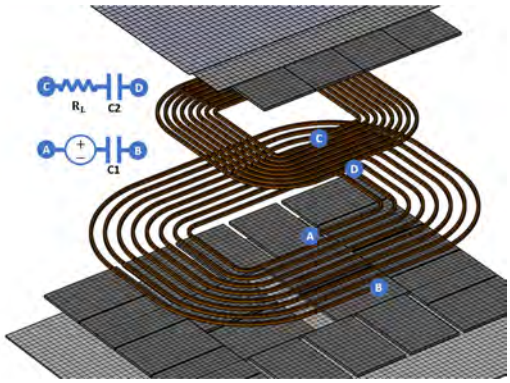


**FIGURE 5.** Sketch of the PEEC model used for the uncertainty quantification electromagnetic/circuit analysis of the WPT2/Z3 system. For the sake of clarity, the model is scaled along the $z$ direction.

distribution, a uniform distribution has to be considered in the provided tolerance range (Category A uncertainty) [53]. In the event that the manufacturer makes the distribution of the measured values on the product samples available, it is possible to assume probability distributions other than the uniform one (Category B uncertainty) [53]. The distribution that is most widely found in these cases is the normal (Gaussian) distribution.

As stated in Section VI, both Gaussian and uniform distribution are considered in this study as they represent, respectively, the best and the worst case scenario in terms of uncertainty probability distribution.

## VI. NUMERICAL METHOD

The electromagnetic problem represented by the study of a WPT system is characterized by several peculiar characteristics. The absence of a well defined magnetic path, typical of most of the standard electric machines, makes the problem an open boundary one. Therefore, if a finite element method based software is used, a wide volume of air should be considered in the simulations. Moreover, the presented analysis requires the coupling of both electromagnetic fields and lumped circuit components.

For these reasons, the PEEC method [37], combined with low–rank compression techniques [54], [55], is particularly suitable for studying the WPT magnetic structure connected with the lumped compensation capacitors, load and voltage excitation. Fig. 5 shows a sketch of the PEEC model of the system (scaled along the $z$ direction to improve the readability) adopted for the numerical studies. PEEC is a particular form of volume integral equation (VIE) method which allows for a natural and useful circuit interpretation of the electromagnetic problem. Thus, connections between discretized objects (i.e. GA and VA assemblies of the WPT device) and lumped circuit components (i.e. the compensation capacitors, load, and voltage excitation) can be easily considered [56]. Moreover, as for all VIE methods, materials with the characteristic of vacuum (i.e. the air) are not discretized, which is a particularly useful feature in the case of WPT devices.

PEEC has already been combined with polynomial chaos expansion (PCE) technique for uncertainty quantifications [57]. However, in this paper, to avoid the issues related to the high computational costs required by PCE techniques, the numerical approach recently proposed in [58] is used instead. Thus, following [58], a parametric model order reduction (PMOR) technique is first applied to the parametric–PEEC WPT problem. Then, as in [58], a Monte Carlo approach is applied to the reduced order model with a very low computational effort. Moreover, to further reduce the computational effort required by the generation of dense matrices, low–rank compression techniques are also applied [54], [56], [59] during the construction of the reduced order model as shown in [58].

It is worth noting that the PMOR approach adopted for the analysis is very general and can be used to study general electromagnetic devices with uncertain material or circuit element parameters. Indeed, as shown in [60], the PMOR/spectral–approximation algorithm can be also applied to the finite element method or the finite integration technique.

## VII. RESULTS AND DISCUSSION

This section presents the results derived by the application of the method described in Section VI on the WPT2 Z3 system adopted as reference. The analysis has been carried out for the maximum and minimum ground clearance values related to the Z3-class (namely $Z3_{\max}$ and $Z3_{\min}$ of Table 3) and the battery voltage values $V_{\text{batt,min}} = 280$ V and $V_{\text{batt,max}} = 420$ V indicated by the SAE J2954 RP. Therefore, four different WPT systems have been considered, i.e. $Z3_{\max}/V_{\text{batt,max}}$, $Z3_{\max}/V_{\text{batt,min}}$, $Z3_{\min}/V_{\text{batt,max}}$, and $Z3_{\min}/V_{\text{batt,min}}$.

The analysis of this section aims at identifying which of the parameters of Table 5 mostly affect the overall behaviour of the four WPT systems defined above. Moreover, it aims at quantifying in what way and to what extent the overall behaviour of the four WPT systems is affected.

### A. NUMERICAL MODEL AND RESULTS

For each of the four WPT systems, tolerances of 5%, 10% and 20% on the compensation capacitors, a tolerance of 20% on the relative permeability of the ferrite plates, and a tolerance of 15% on the aluminum and steel plates have been considered, assuming both uniform and Gaussian probability distributions (the Gaussian distribution has been set so that the 99.7% of data are within three standard deviations of the mean).

For each one of the four WPT systems a PEEC model has been constructed, leading to dense parametric systems with $n_f = 17{,}109$ unknowns (see Fig. 5). A naive Monte Carlo simulation (with $10^6$ samples) applied to the full PEEC problem would have required 48,000 h (indeed, for each Monte Carlo realization, a dense system of size $n_f \times n_f$ must be solved), resulting in a prohibitive computation time.

Therefore, to reduce the computational cost, the PMOR algorithm of [58] has been applied to these four WPT SAE

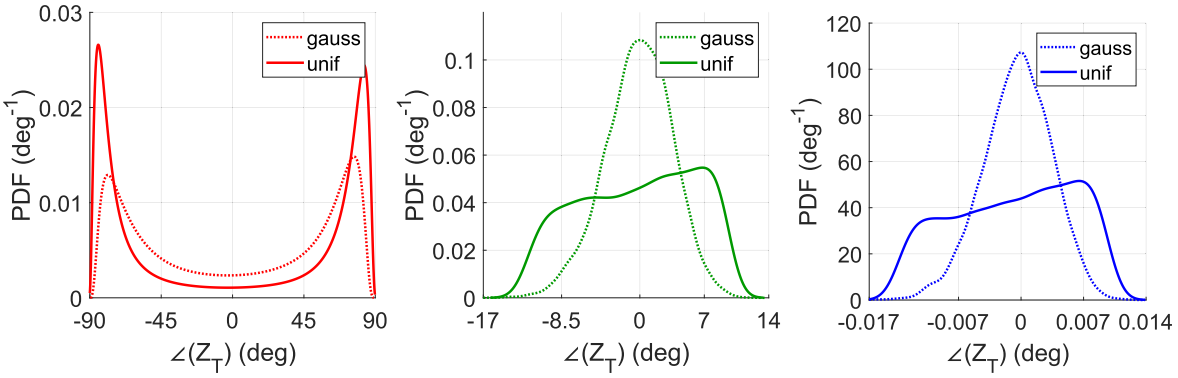


**FIGURE 6.** PDF of the phase of the total impedance $\hat{Z}_T$ at 85 kHz of the SAE J2954 compliant WPT2 Z3 system. Case $Z3_{max}/V_{batt,max}$ (250 mm/420 V). Uncertainties on the two compensation capacitors (20%) only (a). Uncertainties on the two ferrite plates (20%) only (b). Uncertainties on the conductive plates (15%) only (c).

J2954 compliant systems by considering the frequency and all the parameters of Table 5 as nine independent parameters. The frequency range was between 60 kHz to 110 kHz whereas the other variables vary in the ranges of Table 5. Thanks to the PMOR approach [58], [61], the computational complexity of the problem is drastically reduced. Indeed, the PMOR algorithm applied to each of the four WPT systems always led to a reduced order model of size $n_r = 11$, with a tolerance equal to $\eta = 10^{-4}$ for the stop–criterion of the PMOR algorithm (see [58] for more details).

Thanks to the small dimension of the reduced order model and with the aim of extracting probability density functions (PDFs) of quantities of interest for the WPT system (e.g. $\hat{Z}_T$), several Monte Carlo simulations have been performed with a very high number of samples, i.e. $10^6$. Indeed, by using the reduced order model, each realization of a Monte Carlo simulation only requires the solution of a system of size $n_r \times n_r$. Thus, a Monte Carlo simulation (with $10^6$ samples) applied to the reduced order model requires 202 s only. Computation timings are given with respect to a machine equipped with 6-core/24-thread processors (Xeon E5645 at 2.40 GHz) and 104 GB of RAM running Windows.

As stated above, the frequency has been considered as one of the parameters of the reduced order model. Therefore, for a general sample of the parameters of Table 5, the actual resonance frequency of the WPT system can be also detected with a simple bisection method. Therefore, by means of a Monte Carlo simulation, it is also possible to efficiently evaluate the probability density function (PDF) of the resonance frequency of the system.

Several Monte Carlo simulations have been run considering different combinations of the tolerances of the parameters. Thus, several PDFs of quantities which describe the overall behaviour of the WPT system have been obtained.

### B. UNCERTAINTY QUANTIFICATION OF WPT SYSTEMS

The extensive analysis (not entirely reported here for the sake of conciseness) showed that, with respect to all the observed quantities, all the results are between the two edge cases $Z3_{min}/V_{batt,min}$ and $Z3_{max}/V_{batt,max}$. All other results are intermediate compared to those associated with these two cases. Therefore, in the following, results related to $Z3_{min}/V_{batt,min}$ and $Z3_{max}/V_{batt,max}$ are shown.

All the results reported in the following have been obtained by performing 14 Monte Carlo simulations with different simulation conditions. For the sake of clarity, the simulation conditions of such uncertainty quantification analyses are summarised in Table 6. The 7 simulations reported in Table 6 have been computed twice, the first set by imposing a Gaussian PDF and the second one considering a uniform PDF.

As a first result, a preliminary study showed that the tolerances on the conductivities have truly negligible effects on the system performances with respect to the impact of the ferrite permeability and, mostly, the value of the compensation capacitors. In this regard, Fig. 6 shows the PDFs of the phase of $\hat{Z}_T$ when the system works at the fixed frequency of 85 kHz by considering one by one the tolerances on the capacitors (Fig. 6(a) with a tolerance range equal to 20%), ferrite plates (Fig. 6(b)), and conductive plates (Fig. 6(c)) while forcing the others to zero.

A further set of outcomes is summarized through Fig. 7(a) and Fig. 7(b) which show the PDF of the effective resonance frequency of the WPT system. In both graphs, the central dashed line represents the rated frequency of 85 kHz while the other two dashed lines represent the limits of the allowed frequency range, i.e. 79 kHz and 90 kHz, respectively.

Both results clearly show that the limit suggested by the RP can represent a criticality of the WPT system operations. Indeed, this limit can be met with certainty only in the case $Z3_{max}/V_{batt,max}$ and in the presence of a tolerance on capacitor values lower than or equal to 10%, and this if the knowledge on the manufacturing process can indicate a Gaussian distribution of the capacitor values. In all other cases, the mere presence of a tolerance on the capacitors makes it impossible to respect the limits indicated by the RP with

**TABLE 6. Simulation conditions for the uncertainty quantification analyses.**

| Simulation # | $Z3$ | $V_{\text{batt}}$ | Frequency | Tolerances |
|---|---|---|---|---|
| **#1** | $Z3_{\max} = 250$ mm | $V_{\text{batt,max}} = 420$ V | Fixed, 85 kHz | Tolerances of Table 5 |
| **#2** | $Z3_{\max} = 250$ mm | $V_{\text{batt,max}} = 420$ V | variable | Tolerances of Table 5 |
| **#3** | $Z3_{\min} = 170$ mm | $V_{\text{batt,min}} = 280$ V | Fixed, 85 kHz | Tolerances of Table 5 |
| **#4** | $Z3_{\min} = 170$ mm | $V_{\text{batt,min}} = 280$ V | variable | Tolerances of Table 5 |
| **#5** | $Z3_{\max} = 250$ mm | $V_{\text{batt,max}} = 420$ V | Fixed, 85 kHz | Tolerances of Table 5 only for the compensation capacitors |
| **#6** | $Z3_{\max} = 250$ mm | $V_{\text{batt,max}} = 420$ V | Fixed, 85 kHz | Tolerances of Table 5 only for the ferrite plates |
| **#7** | $Z3_{\max} = 250$ mm | $V_{\text{batt,max}} = 420$ V | Fixed, 85 kHz | Tolerances of Table 5 only for the conductive plates |

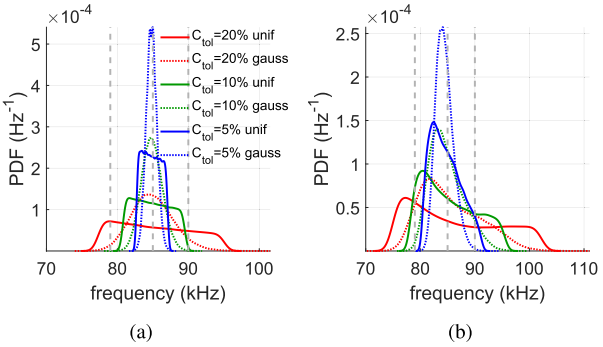


**FIGURE 7.** PDF of the resonance frequency of the SAE J2954 compliant WPT2 Z3 system with uncertainties on the relative magnetic permeability of the two ferrite plates (20%) and on the two compensation capacitors (i.e. 5%, 10%, and 20%). Uniform and normal probability distributions are considered. Case $Z3_{\max}/V_{\text{batt,max}}$ (250 mm/420 V) (a). Case $Z3_{\min}/V_{\text{batt,min}}$ (170 mm/280 V) (b). The central dashed line represents the rated frequency of 85 kHz while the other two dashed lines represent the SAE-limits of the allowed frequency range, i.e. 79 kHz and 90 kHz.

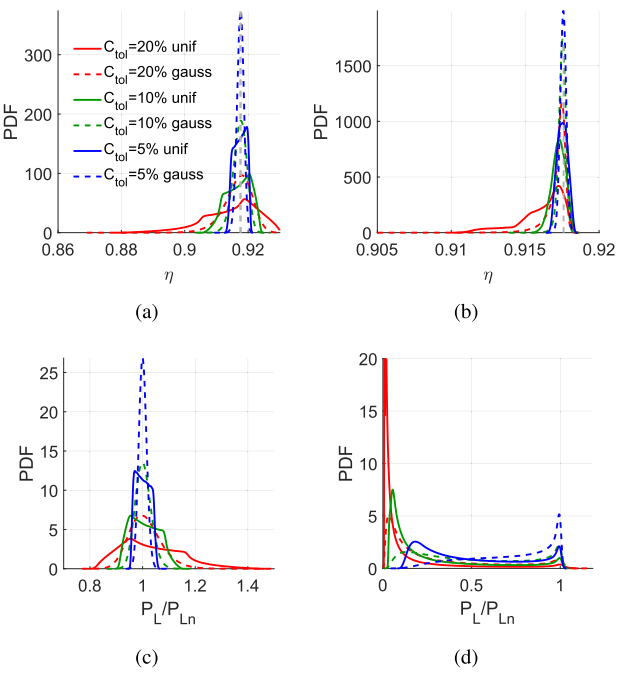


**FIGURE 8.** PDF of $\eta$ and $P_L/P_{Ln}$ of the SAE J2954 compliant WPT2 Z3 system $Z3_{\max}/V_{\text{batt,max}}$ (250 mm/420 V) with uncertainties on the relative magnetic permeability of the two ferrite plates (20%) and on the two compensation capacitors (i.e. 5%, 10%, and 20%) at fixed and variable frequency. Uniform and normal probability distributions are considered. Variable frequency (a) and (c). Fixed frequency (b) and (d).

certainty. In the worst case $Z3_{\min}/V_{\text{batt,min}}$, with a tolerance of 20% on the capacitor values and uniform distribution, there is a 58.70% probability that the system will present the resonance point outside the allowed range (i.e. the portion of area under the solid red curve in Fig. 7(b) which is outside the allowed frequency range is the 58.70% of the total area under the solid red curve). Even in the case of a capacitor with a 5% tolerance, under uniform probability distribution, there is a 3.85% probability that the resonance point will be positioned outside the allowed range. This probability reduces to 0.17% only if a Gaussian distribution can be assumed. Moreover, it is worth noting that, in the $Z3_{\min}/V_{\text{batt,min}}$ case scenario, even for the most favorable value of tolerances, there is a shift in the most probable resonance frequency with respect to the desired nominal value of 85 kHz. In this case in fact, the most probable resonance frequency becomes 83.9 kHz. For the sake of an easier reading, the main probability levels related to the different ranges and distributions of the tolerances inferred from the graphs of Fig. 7, are summarised in Table 7.

As highlighted in the introductory part of the work, the problem of the shift in the effective resonance frequency becomes immediately noticeable in the presence of a variable frequency tuning. Indeed, in this case, the control of the power electronics (i.e. the DC/AC converter of Fig. 1) tries to set the working frequency equal to the actual resonance frequency of the system. This shift in the operating frequency causes the modification of the amplitude of the total impedance of the system and this leads to a variation of the transferred power, and, consequently, of the efficiency, with respect to the ideal case in absence of tolerances. The counterpart represented by the fixed frequency control naturally eliminates the problem of the shifting of the resonance frequency that remains "by-definition" in the allowed range. However, this control does not eliminate the variations in the phase and amplitude of $\hat{Z}_{\text{T}}$ introduced by the presence of tolerances. Hence, also in this case, there is an unavoidable variation in the power transfer capability and efficiency of the energy transfer. The occurrence of this possibility is represented by means of the PDFs shown in Fig. 8 and Fig. 9.

By comparing the results related to the two control techniques, it appears that both of them can maintain the efficiency close to the one in ideal conditions represented by the dashed grey lines in Fig. 8(a), Fig. 8(b), Fig. 9(a) and

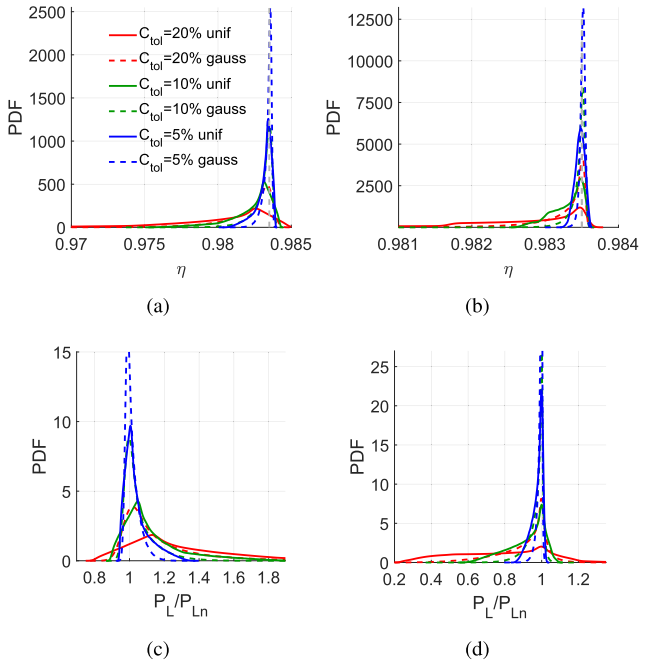


**FIGURE 9.** PDF of $\eta$ and $P_L/P_{Ln}$ of the SAE J2954 compliant WPT2 Z3 system $Z3_{\max}/V_{\text{batt,max}}$ (170 mm/280 V) with uncertainties on the relative magnetic permeability of the two ferrite plates (20%) and on the two compensation capacitors (i.e. 5%, 10%, and 20%) at fixed and variable frequency. Uniform and normal probability distributions are considered. Variable frequency (a) and (c). Fixed frequency (b) and (d).

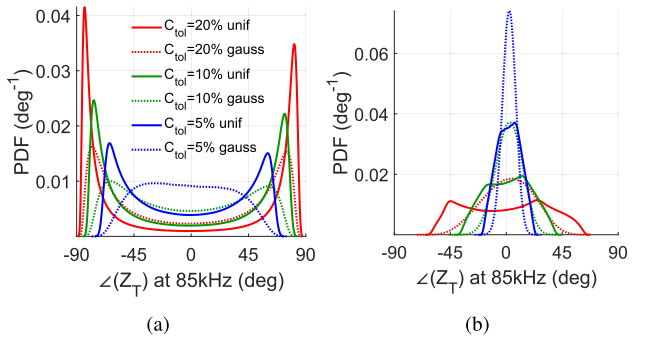


**FIGURE 10.** PDF of the phase of the total impedance $\hat{Z}_T$ at 85 kHz of the SAE J2954 compliant WPT2 Z3 system with uncertainties on the relative magnetic permeability of the two ferrite plates (20%) and on the two compensation capacitors (i.e. 5%, 10%, and 20%). Uniform and normal probability distributions are considered. Case $Z3_{\max}/V_{\text{batt,max}}$ (250 mm/420 V) (a). Case $Z3_{\min}/V_{\text{batt,min}}$ (170 mm/280 V) (b).

Fig. 9(b). In particular, the efficiency under fixed frequency control tends to be affected by a variation of few percentage points while the counterpart under variable frequency tends to reduce to a larger extent. However, the high probability of maintaining high efficiency is not accompanied by an equally high probability of transferring the rated power (i.e. $P_{\text{Ln}}$). This is particularly true for those cases with higher ground clearance, i.e. lower magnetic coupling. The worst case is reached for the case $Z3_{\max}/V_{\text{batt,max}}$ as reported in Fig. 8. In this case, the transfer of the rated power appears to be practically unfeasible and the WPT system under fixed frequency control tends to work with a dramatic reduction of the transferred power.

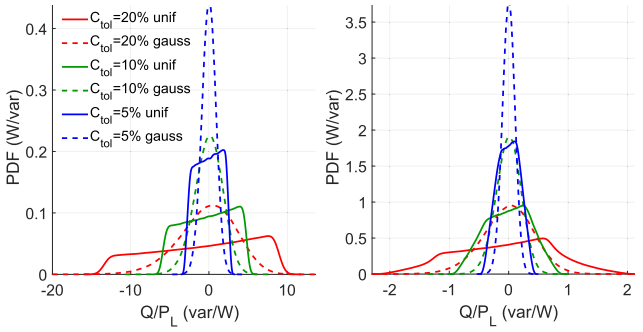


**FIGURE 11.** PDF of the ratio between actual reactive power $Q$ and transmitted power to the load $P_L$ of the SAE J2954 compliant WPT2 Z3 systems $Z3_{\max}/V_{\text{batt,max}}$ (250 mm/420 V) and $Z3_{\min}/V_{\text{batt,min}}$ (170 mm/280 V) with uncertainties on the relative magnetic permeability of the two ferrite plates (20%) and on the two compensation capacitors (i.e. 5%, 10%, and 20%) at fixed frequency. Uniform and normal probability distributions are considered. Case $Z3_{\max}/V_{\text{batt,max}}$ (250 mm/420 V) (a). $Z3_{\min}/V_{\text{batt,min}}$ (170 mm/280 V) (b).

**TABLE 7.** Probability of exceeding SAE frequency limits.

| | $Z3_{\max}/V_{\text{batt,max}}$ | $Z3_{\min}/V_{\text{batt,min}}$ |
|---|---|---|
| $C_{tol} = 20\%$ unif. | 35.19 % | 58.70 % |
| $C_{tol} = 10\%$ unif. | 0.16 % | 27.81 % |
| $C_{tol} = 5\%$ unif. | 0.0065 % | 3.85 % |
| $C_{tol} = 20\%$ gauss | 6.58 % | 31.02 % |
| $C_{tol} = 10\%$ gauss | 0.068 % | 7.37 % |
| $C_{tol} = 5\%$ gauss | 0.0063 % | 0.17 % |

**TABLE 8.** Probability of working with $|Q/P_L| > 0.5$.

| | $Z3_{\max}/V_{\text{batt,max}}$ | $Z3_{\min}/V_{\text{batt,min}}$ |
|---|---|---|
| $C_{tol} = 20\%$ unif. | 95.37 % | 58.58 % |
| $C_{tol} = 10\%$ unif. | 90.69 % | 19.22 % |
| $C_{tol} = 5\%$ unif. | 81.12 % | 0.0064 % |
| $C_{tol} = 20\%$ gauss | 89.10 % | 24.29 % |
| $C_{tol} = 10\%$ gauss | 77.76 % | 1.92 % |
| $C_{tol} = 5\%$ gauss | 57.82 % | 0.0067 % |

The results drawn so far are limited only to the part of the WPT system consisting of the magnetic structure plus the relative compensation capacitors. However, all the variations on the equivalent behavior of the system also have important effects on the power electronics that powers the system. These effects occur only in the case of a fixed frequency control for which the working frequency remains stable at 85 kHz. Referring to the PDFs shown in figure Fig. 10, it is clear how the probability that the phase of $\hat{Z}_T$ remains close to zero is maximum in a few cases only. In the worst case scenario, the probability peak moves towards the extremes. This means that the system becomes with high probability highly inductive or highly capacitive. In both cases this means that the power electronics on the transmitter side has to be designed to manage a significant amount of reactive power, with the PDF shown in Fig. 11, therefore working without the possibility of adopting soft-switching techniques. In particular, the case of capacitive equivalent behavior of the system can become particularly dangerous and requires the adoption of more robust, and more expensive technologies for the switches, such as silicon-carbide switches, in order to be able to operate without risks of damaging the components. In the worst case scenario

(i.e., in this case, case $Z3_{\max}/V_{\text{batt,max}}$) there is a probability of 95.37% that the power electronics is forced to manage a ratio between the reactive power and the actual active power transferred to the load greater or equal to 0.5. This implies that the electronic switches are forced, with extremely high probability, to work under hard-switching conditions. Therefore, they have to be selected with a considerably larger safe operating area with respect to the ones that can be selected if the power electronics is designed to be operated under variable frequency control. Table 8 summarizes the probabilities that the reactive power exceeds the 50% of the amount of transferred active power for the two identified edge cases.

## VIII. CONCLUSION

This work has highlighted how the choice of components, especially the compensation capacitors, is fundamental for the realization of a wireless power transfer (WPT) system that is compliant with the SAE J2954 RP.

Indeed, this choice is not critical for the aluminium and steel elements composing the WPT system. In fact, the results of Section VII-B, have proved that the considered tolerances on the electrical conductivity of the conductive materials have negligible effect on the considered system performances. From the perspective of interoperability of the WPT systems among different vehicles, this aspect represents an important positive outcome because the vehicle floor, that can change from vehicle to vehicle, has a negligible influence on the system behavior. On the contrary, the tolerances on the permeability of the ferrite and on the values of the compensation capacitors have a much more significant impact.

At present, ferrites with tolerances on relative permeability lower than 20% do not seem to be available on the market, therefore the possibility of choosing the tolerances of the components falls exclusively on the capacitors. In this case, the analysis has shown that the construction of a system compliant with the specifications of the SAE J2954 RP requires the use of components with very low production tolerances (roughly lower than 5%) and therefore more expensive. As discussed in Section V, this affects the overall cost in a non–negligible way and may lead to different engineering and market choices.

If components with larger tolerances (that are cheaper and more widely available on the market) are used, the effective resonance frequency of the system drifts to values that are not allowed by the RP, thus making the application non-compliant. This problem can be directly noted if the power electronics supplying the system operates with a variable frequency control. However, even if the fixed frequency control naturally allows respecting the constraint on the frequency set by the RP, this control forces to design the source converter in order to be able to manage reactive power levels comparable with those of the transferred active power. This involves a considerable increase in the cost and size of the electronics.

A possible solution to such problem consists in the use of elements for the tuning of the overall impedance of the system, such as adjustable capacitors or inductors or more complex structures for the electronic tuning [62]. However, these solutions add considerable complexity to the system and, in the case of the tunable passive components, they are not always available at the frequency and power levels of the WPT applications for electric vehicles. A second more easily achievable option consists in the creation of capacitors banks arranged in such a way that the overall tolerance of the assembly is lower. However, this option also increases the cost and complexity of the system.

Finally, from a numerical perspective, it is worth noting that the computational cost of the uncertainty quantification analysis has been drastically reduced thanks to the approach proposed in [58] based on parametric model order reduction.

Future extension of the present work will aim to consider also the presence of tolerances in the geometrical arrangement of the different objects composing the system.

## ACKNOWLEDGMENT

The authors would like to thank prof. A. Carullo of the Department of Electronics and Telecommunications of the Politecnico di Torino, for providing us his valuable advice on the aspects of propagation of the uncertainties faced in this work.

## REFERENCES

[1] K. An, "Battery electric bus infrastructure planning under demand uncertainty," *Transp. Res. C, Emerg. Technol.*, vol. 111, pp. 572–587, Feb. 2020. [Online]. Available: http://www.sciencedirect.com/science/article/pii/S0968090X18314578

[2] M. Abdolmaleki, N. Masoud, and Y. Yin, "Vehicle-to-vehicle wireless power transfer: Paving the way toward an electrified transportation system," *Transp. Res. C, Emerg. Technol.*, vol. 103, pp. 261–280, Jun. 2019. [Online]. Available: http://www.sciencedirect.com/science/article/pii/S0968090X18313676

[3] M. Fuller, "Wireless charging in california: Range, recharge, and vehicle electrification," *Transp. Res. C, Emerg. Technol.*, vol. 67, pp. 343–356, Jun. 2016. [Online]. Available: http://www.sciencedirect.com/science/article/pii/S0968090X16000668

[4] F. He, Y. Yin, and J. Zhou, "Integrated pricing of roads and electricity enabled by wireless power transfer," *Transp. Res. C, Emerg. Technol.*, vol. 34, pp. 1–15, Sep. 2013. [Online]. Available: http://www.sciencedirect.com/science/article/pii/S0968090X1300106X

[5] D. Patil, M. K. McDonough, J. M. Miller, B. Fahimi, and P. T. Balsara, "Wireless power transfer for vehicular applications: Overview and challenges," *IEEE Trans. Transport. Electrific.*, vol. 4, no. 1, pp. 3–37, Mar. 2018.

[6] A. Ahmad, M. S. Alam, and R. Chabaan, "A comprehensive review of wireless charging technologies for electric vehicles," *IEEE Trans. Transport. Electrific.*, vol. 4, no. 1, pp. 38–63, Mar. 2018.

[7] Z. Bi, T. Kan, C. C. Mi, Y. Zhang, Z. Zhao, and G. A. Keoleian, "A review of wireless power transfer for electric vehicles: Prospects to enhance sustainable mobility," *Appl. Energy*, vol. 179, pp. 413–425, Oct. 2016. [Online]. Available: http://www.sciencedirect.com/science/article/pii/S0306261916309448

[8] A. A. S. Mohamed, A. A. Shaier, H. Metwally, and S. I. Selem, "A comprehensive overview of inductive pad in electric vehicles stationary charging," *Appl. Energy*, vol. 262, Mar. 2020, Art. no. 114584. [Online]. Available: http://www.sciencedirect.com/science/article/pii/S0306261920300969

[9] S. Laporte, G. Coquery, V. Deniau, A. De Bernardinis, and N. Hautière, "Dynamic wireless power transfer charging infrastructure for future EVs: From experimental track to real circulated roads demonstrations," *World Electric Vehicle J.*, vol. 10, no. 4, p. 84, Nov. 2019.

[10] J. M. Miller and A. Daga, "Elements of wireless power transfer essential to high power charging of heavy duty vehicles," *IEEE Trans. Transport. Electrific.*, vol. 1, no. 1, pp. 26–39, Jun. 2015.

[11] S. G. Rosu, M. Khalilian, V. Cirimele, and P. Guglielmi, "A dynamic wireless charging system for electric vehicles based on DC/AC converters with SiC MOSFET-IGBT switches and resonant gate-drive," in *Proc. 42nd Annu. Conf. IEEE Ind. Electron. Soc. (IECON)*, Oct. 2016, pp. 4465–4470.

[12] A. Pevere, R. Petrella, C. C. Mi, and S. Zhou, "Design of a high efficiency 22 kW wireless power transfer system for EVs fast contactless charging stations," in *Proc. IEEE Int. Electr. Vehicle Conf. (IEVC)*, Dec. 2014, pp. 1–7.

[13] M. Petersen and F. W. Fuchs, "Development of a 5 kW inductive power transfer system including control strategy for electric vehicles," in *Proc. Eur., Int. Exhib. Conf. Power Electron., Intell. Motion, Renew. Energy Energy Manage., (PCIM)*, 2014, pp. 1–8.

[14] U. K. Madawala, M. Neath, and D. J. Thrimawithana, "A power–frequency controller for bidirectional inductive power transfer systems," *IEEE Trans. Ind. Electron.*, vol. 60, no. 1, pp. 310–317, Jan. 2013.

[15] J. Deng, F. Lu, S. Li, T.-D. Nguyen, and C. Mi, "Development of a high efficiency primary side controlled 7kW wireless power charger," in *Proc. IEEE Int. Electr. Vehicle Conf. (IEVC)*, Dec. 2014, pp. 1–6.

[16] Y. J. Jang, "Survey of the operation and system study on wireless charging electric vehicle systems," *Transp. Res. C, Emerg. Technol.*, vol. 95, pp. 844–866, Oct. 2018. [Online]. Available: http://www.sciencedirect.com/science/article/pii/S0968090X18304649

[17] C. Liu, C. Jiang, and C. Qiu, "Overview of coil designs for wireless charging of electric vehicle," in *Proc. IEEE PELS Workshop Emerg. Technol., Wireless Power Transf. (WoW)*, May 2017, pp. 1–6.

[18] J. L. Villa, J. Sallán, A. Llombart, and J. F. Sanz, "Design of a high frequency inductively coupled power transfer system for electric vehicle battery charge," *Appl. Energy*, vol. 86, no. 3, pp. 355–363, Mar. 2009.

[19] A. N. Azad, A. Echols, V. A. Kulyukin, R. Zane, and Z. Pantic, "Analysis, optimization, and demonstration of a vehicular detection system intended for dynamic wireless charging applications," *IEEE Trans. Transport. Electrific.*, vol. 5, no. 1, pp. 147–161, Mar. 2019.

[20] S. Sinha, A. Kumar, B. Regensburger, and K. K. Afridi, "A new design approach to mitigating the effect of parasitics in capacitive wireless power transfer systems for electric vehicle charging," *IEEE Trans. Transport. Electrific.*, vol. 5, no. 4, pp. 1040–1059, Dec. 2019.

[21] *Wireless Power Transfer for Light-Duty Plug-In/Electric Vehicles and Alignment Methodology*, International Standard SAE J2954, 2019. [Online]. Available: https://www.sae.org/standards/content/j2954_201904/

[22] R. Trinchero, M. Larbi, H. M. Torun, F. G. Canavero, and M. Swaminathan, "Machine learning and uncertainty quantification for surrogate models of integrated devices with a large number of parameters," *IEEE Access*, vol. 7, pp. 4056–4066, 2019.

[23] R. Bosshard and J. W. Kolar, "Multi-objective optimization of 50 kW/85 kHz IPT system for public transport," *IEEE J. Emerg. Sel. Topics Power Electron.*, vol. 4, no. 4, pp. 1370–1382, Aug. 2016.

[24] J. Pries, V. P. N. Galigekere, O. C. Onar, and G.-J. Su, "A 50-kW three-phase wireless power transfer system using bipolar windings and series resonant networks for rotating magnetic fields," *IEEE Trans. Power Electron.*, vol. 35, no. 5, pp. 4500–4517, May 2020.

[25] V. Cirimele, "Design and integration of a dynamic IPT system for automotive applications," Ph.D. dissertation, Politecnico di Torino and Université Paris-Saclay, Turin, Italy, 2017.

[26] W. Zhang and C. C. Mi, "Compensation topologies of high-power wireless power transfer systems," *IEEE Trans. Veh. Technol.*, vol. 65, no. 6, pp. 4768–4778, Jun. 2016.

[27] A. A. S. Mohamed, A. Berzoy, F. G. N. de Almeida, and O. Mohammed, "Modeling and assessment analysis of various compensation topologies in bidirectional IWPT system for EV applications," *IEEE Trans. Ind. Appl.*, vol. 53, no. 5, pp. 4973–4984, Sep. 2017.

[28] K. A. Cota, P. A. Gray, M. Pathmanathan, and P. W. Lehn, "An approach for selecting compensation capacitances in resonance-based EV wireless power transfer systems with switched capacitors," *IEEE Trans. Transport. Electrific.*, vol. 5, no. 4, pp. 1004–1014, Dec. 2019.

[29] M. Ibrahim, L. Pichon, L. Bernard, A. Razek, J. Houivet, and O. Cayol, "Advanced modeling of a 2-kW series–series resonating inductive charger for real electric vehicle," *IEEE Trans. Veh. Technol.*, vol. 64, no. 2, pp. 421–430, Feb. 2015.

[30] A. Bucher and T. Duerbaum, "Analysis and design of a contactless power transmission system based on the extended first harmonic approximation," in *Proc. IEEE Ind. Appl. Soc. Annu. Meeting*, Oct. 2012, pp. 1–7.

[31] S. Bandyopadhyay, V. Prasanth, P. Bauer, and J. A. Ferreira, "Multi-objective optimisation of a 1-kW wireless IPT systems for charging of electric vehicles," in *Proc. IEEE Transp. Electrific. Conf. Expo (ITEC)*, Jun. 2016, pp. 1–7.

[32] V. Cirimele, F. Freschi, and P. Guglielmi, "Wireless power transfer structure design for electric vehicle in charge while driving," in *Proc. Int. Conf. Electr. Mach. (ICEM)*, Sep. 2014, pp. 2461–2467.

[33] B. K. Kushwaha, G. Rituraj, and P. Kumar, "3-D analytical model for computation of mutual inductance for different misalignments with shielding in wireless power transfer system," *IEEE Trans. Transport. Electrific.*, vol. 3, no. 2, pp. 332–342, Jun. 2017.

[34] B. Andreycak. (1999). *Zero Voltage Switching Resonant Power Conversion–Application Note U-138*. Accessed: Oct. 2016. [Online]. Available: http://www.ti.com/lit/an/slua159/slua159.pdf

[35] R. Erickson and D. Maksimovic, *Fundamentals of Power Electronics* (Power Electronics). Cham, Switzerland: Springer, 2001. [Online]. Available: https://books.google.fr/books?id=On9-rJTR8ygC

[36] Q. Zhu, Y. Zhang, C. Liao, Y. Guo, L. Wang, and F. Li, "Experimental study on asymmetric wireless power transfer system for electric vehicle considering ferrous chassis," *IEEE Trans. Transport. Electrific.*, vol. 3, no. 2, pp. 427–433, Jun. 2017.

[37] R. Torchio, "A volume PEEC formulation based on the cell method for electromagnetic problems from low to high frequency," *IEEE Trans. Antennas Propag.*, vol. 67, no. 12, pp. 7452–7465, Jul. 2019.

[38] Collaboration for NDT Education. *Conductivity and Resistivity Values for Aluminum & Alloys*. Accessed: Sep. 1, 2020. [Online]. Available: https://www.nde-ed.org/GeneralResources/MaterialProperties/ET/Conductivity_Al.pdf

[39] Collaboration for NDT Education. *Conductivity and Resistivity Values for Iron & Alloys*. Accessed: Sep. 1, 2020. [Online]. Available: https://www.nde-ed.org/GeneralResources/MaterialProperties/ET/Conductivity_Iron.pdf

[40] M. Budhia, G. A. Covic, and J. T. Boys, "Design and optimization of circular magnetic structures for lumped inductive power transfer systems," *IEEE Trans. Power Electron.*, vol. 26, no. 11, pp. 3096–3108, Nov. 2011.

[41] S. Y. Choi, S. Y. Jeong, B. W. Gu, G. C. Lim, and C. T. Rim, "Ultraslim S-type power supply rails for roadway-powered electric vehicles," *IEEE Trans. Power Electron.*, vol. 30, no. 11, pp. 6456–6468, Nov. 2015.

[42] R. Patel, S. Premkumar, A. Ambade, H. A. Mangalvedhekar, R. N. Rajan, and R. I. Bakhtsingh, "AC resistance calculation of litz wire and its modeling with FEMM," in *Proc. IEEE Int. Conf. Recent Trends Electron., Inf. Commun. Technol. (RTEICT)*, May 2016, pp. 692–696.

[43] V. Cirimele, S. G. Rosu, P. Guglielmi, and F. Freschi, "Performance evaluation of wireless power transfer systems for electric vehicles using the opposition method," in *Proc. IEEE 1st Int. Forum Res. Technol. Soc. Ind. Leveraging Better Tomorrow (RTSI)*, Sep. 2015, pp. 546–550.

[44] J. Winges, T. Rylander, C. Petersson, C. Ekman, L.-A. Johansson, and T. McKelvey, "System identification and tuning of wireless power transfer systems with multiple magnetically coupled resonators," *Trans. Environ. Elect. Eng.*, vol. 2, no. 2, pp. 86–92, 2018.

[45] Y. Yao, Y. Wang, X. Liu, F. Lin, and D. Xu, "A novel parameter tuning method for a double-sided LCL compensated WPT system with better comprehensive performance," *IEEE Trans. Power Electron.*, vol. 33, no. 10, pp. 8525–8536, Oct. 2018.

[46] KEMET Corporation. *Capacitor Selection Guide*. Accessed: Sep. 1, 2020. [Online]. Available: https://www.filcap.de/wp-content/uploads/Gesamtkatalog-KEMET-Capacitor-Selection-Guide.pdf

[47] Alcon Electronics. *General-Purpose-Film-Capacitors-Datasheet-FF-12*. Accessed: Sep. 1, 2020. [Online]. Available: https://alconelectronics.com/wp-content/uploads/2019/11/General-Purpose-Film-Capacitors-Datasheet-FF-12.pdf

[48] T. Diekhans and R. W. De Doncker, "A dual-side controlled inductive power transfer system optimized for large coupling factor variations and partial load," *IEEE Trans. Power Electron.*, vol. 30, no. 11, pp. 6320–6328, Nov. 2015.

[49] X. D. T. García, J. Vázquez, and P. Roncero-Sánchez, "Design, implementation issues and performance of an inductive power transfer system for electric vehicle chargers with series–series compensation," *IET Power Electron.*, vol. 8, no. 10, pp. 1920–1930, Oct. 2015.

[50] Ferroxcube International Holding. *Soft Ferrites and Accessories–Data Handbook*. Accessed: Sep. 1, 2020. [Online]. Available: https://www.ferroxcube.com/en-global/download/download/11

[51] Celem, Power Capacitors. *75kVAr Mica Capacitor for Up to 100MHz and 150 Degrees C*. Accessed: Sep. 1, 2020. [Online]. Available: https://www.celem.com/cp_30_75
[52] R. Ruffo, V. Cirimele, M. Diana, M. Khalilian, A. L. Ganga, and P. Guglielmi, "Sensorless control of the charging process of a dynamic inductive power transfer system with an interleaved nine-phase boost converter," *IEEE Trans. Ind. Electron.*, vol. 65, no. 10, pp. 7630–7639, Oct. 2018.
[53] *Guide to the Expression of Uncertainty in Measurement*, Standard JCGM 100:2008, GUM 1995 With Minor Corrections, ISO/IEC GUIDE 98-3:2008, International Organization for Standardization Standard, Sep. 2010.
[54] D. Voltolina, P. Bettini, P. Alotto, F. Moro, and R. Torchio, "High-performance PEEC analysis of electromagnetic scatterers," *IEEE Trans. Magn.*, vol. 55, no. 6, pp. 1–4, Jun. 2019.
[55] D. Voltolina, R. Torchio, P. Bettini, R. Cavazzana, and M. Moresco, "PEEC modeling of planar spiral resonators," *IEEE Trans. Magn.*, vol. 56, no. 1, pp. 1–4, Jan. 2020.
[56] V. Cirimele, R. Torchio, A. Virgillito, F. Freschi, and P. Alotto, "Challenges in the electromagnetic modeling of road embedded wireless power transfer," *Energies*, vol. 12, no. 14, p. 2677, Jul. 2019.
[57] R. Torchio, L. Di Rienzo, and L. Codecasa, "Stochastic PEEC method based on polynomial chaos expansion," *IEEE Trans. Magn.*, vol. 55, no. 6, pp. 1–4, Jun. 2019.
[58] R. Torchio, L. Codecasa, L. Di Rienzo, and F. Moro, "Fast uncertainty quantification in low frequency electromagnetic problems by an integral equation method based on hierarchical matrix compression," *IEEE Access*, vol. 7, pp. 163919–163932, 2019.
[59] R. Torchio, P. Bettini, and P. Alotto, "PEEC-based analysis of complex fusion magnets during fast voltage transients with H-matrix compression," *IEEE Trans. Magn.*, vol. 53, no. 6, pp. 1–4, Jun. 2017.
[60] L. Codecasa and L. Di Rienzo, "MOR-based approach to uncertainty quantification in electrokinetics with correlated random material parameters," *IEEE Trans. Magn.*, vol. 53, no. 6, pp. 1–4, Jun. 2017.
[61] F. Y. Lin, C. Carretero, G. A. Covic, and J. T. Boys, "A reduced order model to determine the coupling factor between magnetic pads used in wireless power transfer," *IEEE Trans. Transport. Electrific.*, vol. 3, no. 2, pp. 321–331, Jun. 2017.
[62] S. Aldhaher, P. C.-K. Luk, and J. F. Whidborne, "Electronic tuning of misaligned coils in wireless power transfer systems," *IEEE Trans. Power Electron.*, vol. 29, no. 11, pp. 5975–5982, Nov. 2014.

**VINCENZO CIRIMELE** (Member, IEEE) was born in Verbicaro, Italy, in 1987. He received the M.Sc. degree in electrical engineering and the Ph.D. degree in electronics engineering from the Politecnico di Torino, Italy, and the Ph.D. degree in electrical engineering from the Université Paris-Saclay, France, in February 2017. He is currently enrolled as an Assistant Professor with the Department of Energy, Politecnico di Torino. His research interests include protection of people from the magnetic field at industrial frequency, electromagnetic modeling, and inductive power transmission for electric vehicles.

**RICCARDO TORCHIO** was born in Padova, Italy, in 1992. He received the M.S. degree in electrical engineering from the University of Padova, Padova, in 2016, and the Ph.D. degree in electrical engineering from the University of Padova and the Grenoble Electrical Engineering Laboratory (G2ELab), Université Grenoble Alpes, France, in December 2019. He is currently working with the University of Padova as a Postdoctoral student at the project "Towards the all-electric vehicle: Numerical design tools for safety and security." His research interests include numerical methods, low-rank compression techniques, uncertainty quantifications, wireless power transfer applications, model order reduction, model predictive control, and the development of integral formulations for the study of low and high frequency electromagnetic devices.

**JUAN LUIS VILLA** was born in Zaragoza, Spain, in 1966. He received the M.E. and Ph.D. degrees in industrial engineering from the University of Zaragoza, Zaragoza, in 1997 and 2009, respectively. He is currently a Researcher in energy engineering with the Centre of Research for Energy Resources and Consumption (CIRCE) and a Lecturer with the Electrical Engineering Department, University of Zaragoza. His research interests include wireless power transfer, power electronics, electric vehicles, and renewable energy integration.

**FABIO FRESCHI** (Senior Member, IEEE) received the Laurea degree *(summa cum laude)* in electrical engineering from the Politecnico di Torino, Torino, Italy, in 2002, and the Ph.D. degree and the European Doctorate degree in electrical engineering, in April 2006. From 2003 to 2005, he attended the Doctorate School at the Electrical Engineering Department, Politecnico di Torino. In 2006, he was a Visiting Researcher with the Technical University of Graz, Graz, Austria. From January 2005 to July 2007, he was a Research Assistant with the Electrical Engineering Department, Politecnico di Torino. In 2013, he was a Visiting Academic with The University of Queensland, Brisbane, QLD, Australia. He is currently an Associate Professor in fundamentals of electrical engineering with the Politecnico di Torino. His research and scientific interests include numerical modeling and computation of electromagnetic and bioelectromagnetic fields. Part of his activity is related to the study and development of deterministic and stochastic optimization algorithms applied to the study of electromagnetic devices and complex energy systems. He authored more than 100 conference and journal papers in these fields. He is an investigator of several national and international research projects. He is the Chair of the IEEE IAS Power Systems Engineering Committee and an Associate Editor for the same Society. He acts as a referee of many international journals in the field of numerical electromagnetics, optimization, and operational research.

**PIERGIORGIO ALOTTO** (Senior Member, IEEE) was born in Genoa, Italy, in 1968. He received the degree (Hons.) in electrical engineering from the University of Genoa, in 1992, and the Ph.D. degree in electrical engineering from the University of Genoa, in 1997. From 1992 to 1994, he was employed by the Vector Fields Ltd., a scientific software house, Oxford, U.K., as a Software Development Engineer. From 1997 to 2005, he served as an Assistant Professor with the University of Genoa. Since 2005, he has been with the University of Padua, Italy, where, since 2018, he has been a Full Professor of electrical engineering. His scientific interests which have led to over 150 indexed publications in peer-reviewed international journals and conference proceedings include several aspects of the computation of electromagnetic fields and the design of electromagnetic devices. He is inventor of three national patents (one with PCT extension) concerning an electrostatic purification filter, a magnetic differential gear, and a battery operated system for the logging industry.

**LORENZO CODECASA** (Senior Member, IEEE) received the Ph.D. degree in electronic engineering from Politecnico di Milano, in 2001. From 2002 to 2010, he worked as an Assistant Professor of electrical engineering with the Department of Electronics, Information, and Bioengineering, Politecnico di Milano. Since 2010, he has worked as an Associate Professor of electrical engineering in the same department. His main research contributions are in the theoretical analysis and in the computational investigation of electric circuits and electromagnetic fields. In his research on heat transfer and thermal management of electronic components, he has introduced original industrial-strength approaches to the extraction of compact thermal models, currently available in commercial software. For these activities, in 2016, he received the Harvey Rosten Award for Excellence. He has been serving as an Associate Editor of the IEEE TRANSACTIONS OF COMPONENTS, PACKAGING AND MANUFACTURING TECHNOLOGY. In 2019, he served as a Program Chair of the conference THERMal INvestigation of Integrated Circuits (THERMINIC). In his research areas, he has authored or coauthored over 190 papers in refereed international journals and conference proceedings.

**LUCA DI RIENZO** (Senior Member, IEEE) received the Laurea (M.Sc.) degree *(cum laude)* and the Ph.D. degree in electrical engineering from Politecnico di Milano, in 1996 and 2001, respectively. He is currently an Associate Professor with the Dipartimento di Elettronica, Informazione e Bioingegneria, Politecnico di Milano. His current research interests are in the field of computational electromagnetics and include magnetic inverse problems, integral equation methods, surface impedance boundary conditions, and uncertainty quantification. He is an Associate Editor-in-Chief of *The Applied Computational Electromagnetics Society Journal* and a member of the Editorial Board of *Sensing and Imaging* and of *COMPEL-The International Journal for Computation and Mathematics in Electrical and Electronic Engineering*.